

Article

Phytogenic Fabrication of Copper Oxide Nanoparticles for Antibacterial and Antioxidant Screening: Physico-Chemical Study

Fazal Ur Rehman¹, Rashid Mahmood¹, Sirajul Haq^{1,*}, Pervaiz Ahmad², Salah Ud Din¹,
Mayeen Uddin Khandaker³, Abubakr M. Idris^{4,5} and Ivar Zekker⁶

¹ Department of Chemistry, University of Azad Jammu and Kashmir, Muzaffarabad 13100, Pakistan

² Department of Physics, University of Azad Jammu and Kashmir, Muzaffarabad 13100, Pakistan

³ Centre for Applied Physics and Radiation Technologies, School of Engineering and Technology, Bandar Sunway 47500, Selangor, Malaysia

⁴ Department of Chemistry, College of Science, King Khalid University, Abha 61421, Saudi Arabia

⁵ Research Center for Advanced Materials Science (RCAMS), King Khalid University, Abha 61421, Saudi Arabia

⁶ Institute of Chemistry, University of Tartu, Ravila 14a, 50411 Tartu, Estonia

* Correspondence: cii_raj@yahoo.com

Abstract: *Bergenia ciliata* (*B. ciliate*) leaf extract was used as a capping and stabilizing agent to synthesize copper oxide nanoparticles (CuO NPs). The selection of *B. ciliate* is purely based on its rich phytochemical composition and less utilization in green chemistry. The X-ray diffraction (XRD) analysis showed that the CuO NPs were found to be highly crystalline, while the irregular morphology and other structural properties were investigated by scanning electron microscopy (SEM) and transmission electron microscopy (TEM), and the average particle size was found to be 50.05 nm. Energy dispersive X-ray (EDX) spectroscopy was used to determine the percentage composition and purity, whereas Fourier transform infrared (FTIR) spectroscopy was utilized to examine the surface functional groups. CuO NPs were tested for their antibacterial properties against Gram-positive and Gram-negative bacteria, and the activity was found to increase with an increasing concentration of CuO NPs in the wells. The dose-dependent antioxidant potential is slightly higher than ascorbic acid.

Keywords: copper oxide; morphology; crystalline; microscopy



Citation: Rehman, F.U.; Mahmood, R.; Haq, S.; Ahmad, P.; Din, S.U.; Khandaker, M.U.; Idris, A.M.; Zekker, I. Phytogenic Fabrication of Copper Oxide Nanoparticles for Antibacterial and Antioxidant Screening: Physico-Chemical Study. *Crystals* **2022**, *12*, 1796. <https://doi.org/10.3390/cryst12121796>

Academic Editor: Marian Valko

Received: 25 September 2022

Accepted: 5 December 2022

Published: 9 December 2022

Publisher's Note: MDPI stays neutral with regard to jurisdictional claims in published maps and institutional affiliations.



Copyright: © 2022 by the authors. Licensee MDPI, Basel, Switzerland. This article is an open access article distributed under the terms and conditions of the Creative Commons Attribution (CC BY) license (<https://creativecommons.org/licenses/by/4.0/>).

1. Introduction

The improper and wide utilization of antibiotics led to the formation of multi-drug resistant bacterial strains, which are considered a serious threat to human health. To tackle these strains, multiple drugs are required. These medications are quite expensive, take a long time to work, and may cause side effects [1]. Similarly, different chemical entities that include one or more unpaired electrons are known as free radicals. These very unstable molecules inflict harm on other molecules by removing electrons from them in an attempt to achieve stability. They arise inside the system and are highly reactive, posing a threat to the short-lived chemical species [2,3]. To deal with these multiple problems, a single-step solution is inorganic nanomaterials (metals/metal oxides), which have attracted attention due to their safe and stable nature as compared to organic materials [4–7].

The CuO NPs is a p-type semiconductor that has a low band gap of 1.2 eV, and exhibits unique optical, electrical, mechanical, magnetic, and chemical capabilities [8,9]. CuO NPs are frequently used as transistors in the design and manufacture of batteries, sensors, solar cells, solar energy conversion devices, high-temperature superconductors, heterogeneous catalysts, drug delivery agents, imaging agents antibacterial and antioxidant agent [10–12]. CuO is less costly than silver and gold NPs, both of which have significant antibacterial properties and have exceedingly unique crystal morphologies and large surface areas when produced, making those potentially highly important antibacterial

agents [13,14]. By comparing Cu with other metals such as Zn and Fe, essential trace elements are needed to regulate various biological processes within living organisms. The nano-sized oxides of these metals possess widespread applications in many areas, among which the therapeutic potentials of these metal oxides are of great public concern [15]. CuO, on the other hand, has a lower toxicity level toward organisms and a higher therapeutic efficacy when compared to other metal oxides such as zinc oxide and iron oxide [16,17]. When compared to organic antibacterial agents, these NPs are more durable and stable with an extended shelf life [18,19].

CuO NPs have been synthesized using a variety of processes including chemical, physical, photochemical, and electrochemical procedures [20]. Although most of these methods are effective in the fabrication of pure and well-defined NPs, though, they are either expensive or environmentally hazardous [21]. Green fabrication is a sophisticated alternative to traditional methods and has received a lot of interest in the last few years due to its simple, cost-effective, and environmentally friendly nature [22]. It not only disregards the use of toxic chemicals but also allows for the active coating of biological substances on the surface of the NPs [23]. The usage of plant extract for NPs production is a rapidly developing research topic referred to as the green synthesis of NPs [24]. Plant-based CuO NPs synthesis is presently under development and according to a literature survey, there are just a limited number of publications on the plant-mediated synthesis of CuO NPs [25]. The CuO NPs were synthesized using plant extracts such as *Aloe vera* leaves extract [25], *Carcia papaya* leaves extract [18], *Centella asiatica* leaf extract [20], *Malva sylvestris* leaves extract, *Ocimum basilicum* extract [22], *Gloriosa superba* plant extract [26], *Populus ciliata* leaves extract [27], *Fumaria indica* plant extract [28] which showed the NP formation of different sizes and morphologies such as quasi-spherical, spherical, rod-shaped, hexagonal with agglomerates. In most studies, the CuO NPs synthesized via the green route are used either for antibacterial or antioxidant applications, however, in this, both antibacterial and antioxidant potentials of the CuO NPs were explored in a dose-dependent manner.

The goal of this study is to use *B. ciliata* medicinal plant leaves extract as a bio-reductant and capping agent to synthesize CuO NPs. *B. ciliata* leaf extract is rich in phytochemicals that are responsible for CuO NPs reduction and biofabrication. Several approaches were employed to characterize the CuO NPs made using the biogenic process. The antioxidant and antibacterial activities of the CuO NPs as produced were also investigated.

2. Materials and Methods

2.1. Reagents

All the reagents used in this experiment including copper sulfate penta-hydrated ($\text{CuSO}_4 \cdot 5\text{H}_2\text{O}$), (2,2'-Azino-bis(3-ethylbenzothiazoline-6-sulfonic acid) diammonium salt (ABTS), Agar nutrient, potassium persulphate were of analytical grade and bought from Merck and Sigma-Aldrich.

2.2. Collections of Plant Leave and Extract Preparation

B. ciliata leaves were collected from Neelum Valley, Azad Jammu, and Kashmir, Pakistan, and were all washed many times with distilled water to eliminate the dust particles before being used in the experiment. Afterward, the plant leaves were shade dried for seven days to remove the moisture and then boiled at 80 °C for 30 min in 200 mL of distilled water. After cooling the mixture to room temperature and was filtered with the help of Whatman No.1 filter paper and kept at 4 °C as stock extract for the production of CuO NPs.

2.3. Phytochemical Synthesis of CuO NPs

The 70 mL of copper sulfate penta-hydrated ($\text{CuSO}_4 \cdot 5\text{H}_2\text{O}$) was combined with 30 mL of an aqueous leaves extract of *B. ciliata* with continual stirring on magnetic stirring at 70 °C to prepare CuO NPs. The color changes from deep blue to brick red with increasing time duration indicating formation of the CuO NPs. The precipitate formed was collected through centrifugation at 4000 rpm for 30 min and then washed thrice with distilled water.

The solid product was dried in an oven at 100 °C and was then calcined at 400 °C for 2 h in the muffle furnace.

2.4. Instrumentation

The physico-chemical properties of synthesized CuO NPs prepared by green method were studied through different techniques as is also evident from the literature [29,30]. The crystallite geometry and size of synthesized CuO NPs were studied via Philips X'Pert XRD (manufactured by CAE, Montreal, Canada) using 40 kV, 30 mA, Cu K α radiation ($\lambda = 1.54.5 \text{ \AA}$) with scan speed of $2\theta = 5 \text{ min}^{-1}$. The morphology was examined using a HITACHI HT-780 TEM (Cleveland, TN, USA) with accelerating voltage of 100 kV. EDX and SEM were performed using a JEOL JSM-5600LV scanning electron microscope (Yokogishi, Tokyo, Japan). FTIR spectrum was obtained with Bruker spectrometer ranging between 4000–400 cm^{-1} using KBr pellets.

2.5. Bactericidal Assay

The antibacterial effectiveness of CuO NPs was assessed against *Staphylococcus aureus* (*S. aureus*) ATCC# 5638 and *Escherichia coli* (*E. coli*) ATCC# 15,224 using the agar well diffusion method [31]. The plates were created using DW and agar materials, and they were let to set up at room temperature. The medium was covered with the overnight developed bacterial culture and the wells were drilled with a polystyrene tip. The stock suspension was created by ultrasonically dispersing 50, 100, 500, and 1000 μg of CuO NPs in 1 mL of DW, and then a volume of 100 μL was added to each well. Following a 24 h incubation period at 37 °C, the zone of inhibition, which indicates the activity of the CuO NPs, was measured in millimeters (mm).

2.6. ABTS \bullet^+ Scavenging Assay

A previously reported method was used for the screening of CuO NPs against the ABTS free radicals [32]. First, the ABTS \bullet^+ was created by combining a 5 mM solution of K₂S₂O₈ with 14 mM ABTS (1:1 (*v/v*) and 12:8 (*w/w*)) in the dark. The absorbance was then measured at 734 nm after sixteen hours. Amounts of 5, 25, 50, 100, 200, and 400 μg of CuO NPs were dispersed in 1 mL of distilled water using ultrasonic dispersion for 30 min at room temperature. After combining 0.15 mL of the ABTS+ solution with 0.2 mL of the CuO NPs suspension, the absorbance was measured after 30 min. The activity of CuO NPs is defined as the decrease in absorbance, and the current activity was estimated using Equation (1), where A_0 and A_i are the control absorbance and absorbance, respectively.

$$\%RSA = \left[\left(\frac{A_0 + A_i}{A_0} \right) \right] \times 100 \quad (1)$$

3. Results

3.1. XRD Analysis

XRD pattern of CuO NPs produced with *B. ciliate* leaves extract is shown in Figure 1. In order to examine the crystal structure of CuO NPs, XRD analysis was performed, and the peaks were found at 32.50, 35.63, 38.77, 46.69, 48.83, 51.47, 53.87, 58.04, 61.54, 65.66, 66.49, 68.31, 72.60, 75.07, and 80.35, with corresponding hkl values of $-110, 002, 111, -112, -202, 112, 020, 202, -113, 022, -311, -220, 311, 004,$ and -204 . These diffraction peaks are due to the monoclinic geometry-shaped CuO crystallite, which was compared to the standard powder diffraction card of JCPDS no. 00-045-0937. Using full width at half maximum (FWHM) data, calculated average crystallite size 48 nm. The sharp diffraction peaks that appeared in the XRD pattern suggest the formation of highly crystalline CuO NPs. All the observed peaks are assigned to monoclinic CuO, which also suggests the formation of extremely favorable and single-phase CuO crystallites.

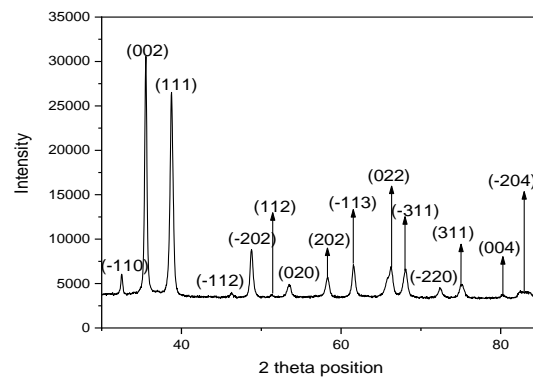


Figure 1. XRD Spectrum of *B. ciliate* mediated CuO NPs.

3.2. SEM Analysis

The SEM images of the synthesized CuO NPs shown in Figure 2, show that the particles are haphazardly dispersed forming a porous network with several cavities of different sizes and shapes in between. Both the low (a) and high (b) magnified SEM images show nearly identical morphology of the sample. The particles are closely connected with one another, and in some areas of the micrographs, the boundaries between the particles disappeared. However, some individual particles are also seen in the images, which are of different shapes and sizes. Due to the high degree of agglomeration, the precise size and morphology of the particles are difficult to determine.

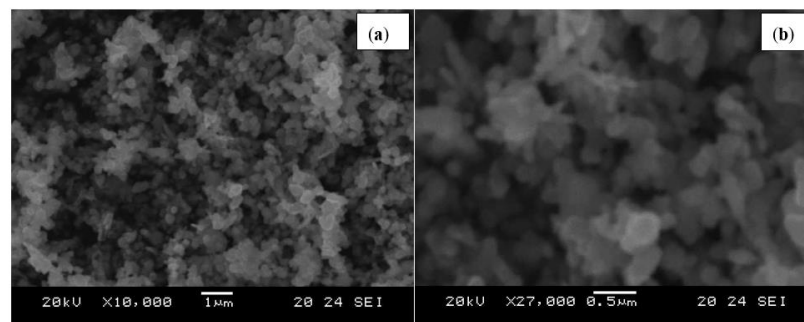


Figure 2. Low (a) and High (b) magnification SEM images of *B. ciliate* mediated CuO NPs.

3.3. TEM Analysis

The low- and high-magnification TEM images provided further insights into the morphology and particle size distribution profiles of CuO NPs (Figure 3a,b). Both the TEM images' low resolution (80,000 \times) and high resolution (120,000 \times) show that the particles are closely connected with each other, and the boundaries of the particles are visible. The particles seem to be unevenly distributed in both images. In both images, irregular morphological-shaped particles are seen, where some particles possess a slightly elongated shape, whereas others have nearly rectangular and square-type structures. The left lower portion of the low magnification image is highly agglomerated and a compact structure has formed the accumulation of eight to ten smaller particles. The particles range from 64.85 to 121.29 nm with an average size of 69.15 nm.

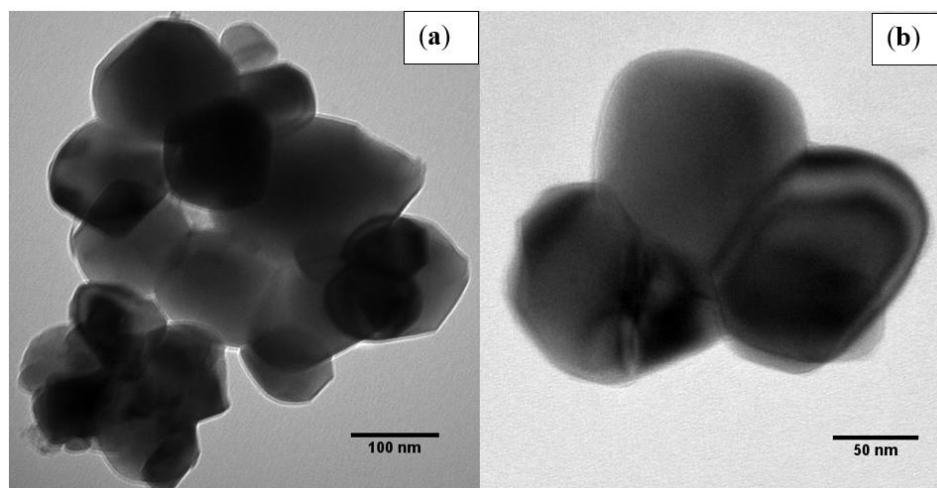


Figure 3. Low (a) and High (b) magnification TEM images of *B. ciliate* mediated CuO NPs.

3.4. EDX and FTIR Analysis

The elemental composition was analyzed through EDX and obtained spectrum confirmed the existence of copper and oxygen in the synthesized CuO NPs (Figure 4a). The weight percent of the copper and oxygen detected in the prepared CuO NPs is 71.74 and 28.36, respectively, and are found very close to that reported in the literature [33]. The chemical composition was studied through FTIR, and the spectrum obtained is shown in (Figure 4b). The low-intensity peak at 1118.19 cm^{-1} is due to O-Cu-O bond vibrations in the lattice structure whereas the intense peak at 452.48 cm^{-1} specifies Cu-O vibrations that indicate the formation of CuO NPs [34,35]. The presence of no other peak in both (EDX and FTIR spectra) confirmed the formation of highly pure CuO NPs. That means that the EDX and FTIR results are in good agreement with the XRD results regarding the purity of the prepared CuO NPs.

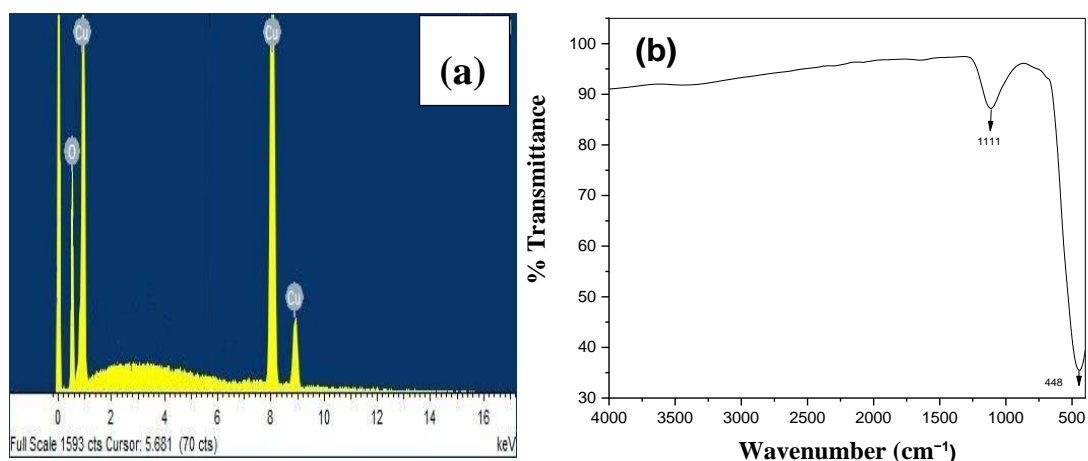


Figure 4. EDX spectrum (a) and FTIR spectrum (b) of *B. ciliate* mediated CuO NPs.

3.5. Antibacterial Activity

Figure 5 shows the antibacterial activity of the CuO NPs and the inhibitory zone displayed by CuO NPs at various doses ($50\text{ }\mu\text{g/mL}$, $100\text{ }\mu\text{g/mL}$, $500\text{ }\mu\text{g/mL}$, $1000\text{ }\mu\text{g/mL}$) against bacterial pathogens (*S. aureus* and *E. coli*). Zones were measured in millimeters (mm) around each well and the size of the zones of inhibition increased as the concentration increased as shown in Table 1. The activity was found to increase with increasing concentration of the CuO NPs in the wells and higher activity was found against *E. coli* compared to *S. aureus*. The difference in the activity is attributed to the difference in the

cell wall composition, which affects the penetration of NPs into bacterial cells, and also due to the difference in the surface charge of both bacteria. The metal cation and other radicals released in an aqueous solution are highly reactive and link the bacteria via surface negative charge and thiol groups. Bacterial cell death occurs when more copper cations engage with the bacterial surface and thiol groups [36]. CuO NPs interfere with bacteria's biological mechanisms by reducing cell growth, resulting in a bactericidal effect [37]. Bacterial death can be caused by NPs deposition on the surface of bacteria and infiltration into the cytoplasm. By producing other reactive species from NPs and then penetrating bacteria, reactive oxygen species can damage cellular constitutions (lipids, peptidoglycan) and induce cell inactivation [38]. In comparison to *S. aureus*, *E. coli* is more sensitive to CuO NPs due to a strong surface negative charge and thin peptidoglycan layer. Because the *S. aureus* cell wall is made up of thick and tough peptidoglycan, it is difficult for the CuO NPs to penetrate inside. In contrast, the *E. coli* cell wall is comparatively soft having a thin layer of peptidoglycan, which permits the infiltration of the incoming antibacterial agent that disturbs the cytoplasmic composition and triggers cell death [39].



Figure 5. Pictorial representation of the antibacterial activity of *B. ciliate* mediated CuO NPs.

Table 1. Antibacterial activity of CuO NPs against *E. coli* and *S. aureus* and zones of inhibition was measured in millimeters (mm).

Microorganisms	Zones of Inhibition (mm) at Different Concentrations				Variance (S ²)	STD Deviation (S)	Correlation b/w Dose and Activity	PC	NC
	50 (µg/mL)	100 (µg/mL)	500 (µg/mL)	1 (mg/mL)					
<i>E. coli</i>	5	8	13	19	3.00	1.74	0.08	24	00
<i>S. aureus</i>	3	5	10	16	3.78	1.95	0.07	21	00

3.6. Antioxidant Activity

The ABTS radical scavenging activity of the produced CuO NPs to scavenge radicals was tested using the ABBS assay. The findings of free radical scavenging activity at various concentrations of CuO NPs were examined and compared to ascorbic acid used as standard antioxidants and the obtained results are tabulated in Table 2. The decrease in the absorbance at 734 nm with increasing concentrations is attributed to the antioxidant potential of the CuO NPs. The percent radical scavenging activity of CuO NPs is increased

with increasing concentration. At varied concentrations, CuO NPs showed scavenging activity ranging from 22.62 percent to 85.27 percent. The increasing radical scavenging potential is due to the oxygen atom which transfers the electron density to the ABTS radical cation and stabilizes it. The IC₅₀ value is the concentration of antioxidants that can neutralize 50 percent of the ABTS^{•+} radicals and is found to be 110.50 percent for CuO NPs and ascorbic acid is 171.04 percent. The lower IC₅₀ value for the CuO NPs compared to the standard are suggest the high efficacy of the synthesized antioxidant as compared to the standard antioxidant [40].

Table 2. Antioxidant activity of CuO NPs against ABTS free radicals and statistical analysis.

Sample	Concentration (µg/mL)	%RSA	IC ₅₀ (µg/mL)	Variance (S ²)	Std Deviation (S)	Correlation Constant b/w Dose and %RSA
CuO NPs	5	22.62	110.50	2.82	1.68	0.97
	25	30.36				
	50	44.83				
	100	59.27				
	200	73.01				
	400	88.27				
Ascorbic acid	5	14.1	171.04	3.71	1.93	0.78
	25	22.15				
	50	34.13				
	100	47.83				
	200	64.98				
	400	78.39				

4. Conclusions

The plant leaf extract-assisted synthesis is a fast, environmentally friendly, one-pot synthesis, simple, clean, energy-saving, and economically feasible way for the production of CuO NPs, which can also be used for the synthesis of other NPs as well. The physico-chemical study reveals that the produced CuO NPs are extremely pure, highly crystalline, and a bit irregular in size and morphology shape, and can be used for many applications in the future. The antibacterial and antioxidant activities are seen to increase with increasing CuO NPs in the experiment. The antibacterial activity of CuO NPs was high against *E. coli* as compared to *S. aureus*; however, the activity of CuO NPs against both bacterial species is less than the standard drug. The low IC₅₀ value for CuO NPs as compared to ascorbic acid highlights the importance of this study.

Author Contributions: Conceptualization, S.H. and R.M.; methodology, R.M. and S.H.; software, P.A. and S.U.D.; validation, P.A., M.U.K. and A.M.I.; formal analysis, F.U.R. and S.U.D.; investigation, F.U.R. and M.U.K.; resources, S.H. and A.M.I.; data curation, I.Z.; writing—original draft preparation, F.U.R., S.U.D. and I.Z.; writing—review and editing, P.A., M.U.K. and I.Z.; visualization, I.Z.; supervision, R.M. and S.H.; project administration, A.M.I.; funding acquisition, A.M.I. All authors have read and agreed to the published version of the manuscript.

Funding: This research was funded by the Deanship of Scientific Research at King Khalid University, Saudi Arabia, grant number 39/43.

Institutional Review Board Statement: Not applicable.

Informed Consent Statement: Not applicable.

Data Availability Statement: All the data are enclosed in the manuscript.

Acknowledgments: The authors extend their appreciation to the Deanship of Scientific Research at King Khalid University, Saudi Arabia, for funding this work through Large Group Research Project under grant number 39/43 and the Research Center of Advanced Materials at King Khalid University, Saudi Arabia for their valuable technical support.

Conflicts of Interest: The authors declare no conflict of interest.

References

1. Hajipour, M.J.; Fromm, K.M.; Akbar Ashkarran, A.; de Jimenez Aberasturi, D.; de Larramendi, I.R.; Rojo, T.; Serpooshan, V.; Parak, W.J.; Mahmoudi, M. Antibacterial properties of nanoparticles. *Trends Biotechnol.* **2012**, *30*, 499–511. [[CrossRef](#)] [[PubMed](#)]
2. Fouda, A.; Hassan, S.E.D.; Abdo, A.M.; El-Gamal, M.S. Antimicrobial, Antioxidant and Larvicidal Activities of Spherical Silver Nanoparticles Synthesized by Endophytic *Streptomyces* spp. *Biol. Trace Elem. Res.* **2020**, *195*, 707–724. [[CrossRef](#)] [[PubMed](#)]
3. Kazemi, M.; Akbari, A.; Sabouri, Z.; Soleimanpour, S.; Zarrinfar, H.; Khatami, M.; Darroudi, M. Green synthesis of colloidal selenium nanoparticles in starch solutions and investigation of their photocatalytic, antimicrobial, and cytotoxicity effects. *Bioprocess Biosyst. Eng.* **2021**, *44*, 1215–1225. [[CrossRef](#)] [[PubMed](#)]
4. Sawai, J. Quantitative evaluation of antibacterial activities of metallic oxide powders (ZnO, MgO and CaO) by conductimetric assay. *J. Microbiol. Methods* **2003**, *54*, 177–182. [[CrossRef](#)] [[PubMed](#)]
5. Kazemi, M.; Akbari, A.; Zarrinfar, H.; Soleimanpour, S.; Sabouri, Z.; Khatami, M.; Darroudi, M. Evaluation of Antifungal and Photocatalytic Activities of Gelatin-Stabilized Selenium Oxide Nanoparticles. *J. Inorg. Organomet. Polym. Mater.* **2020**, *30*, 3036–3044. [[CrossRef](#)]
6. Bafghi, M.H.; Nazari, R.; Darroudi, M.; Zargar, M.; Zarrinfar, H. The effect of biosynthesized selenium nanoparticles on the expression of CYP51A and HSP90 antifungal resistance genes in *Aspergillus fumigatus* and *Aspergillus flavus*. *Biotechnol. Prog.* **2022**, *38*, e3206. [[CrossRef](#)]
7. Abdelfatah, M.; Salah, H.Y.; EL-Henawey, M.I.; Oraby, A.H.; El-Shaer, A.; Ismail, W. Insight into Co concentrations effect on the structural, optical, and photoelectrochemical properties of ZnO rod arrays for optoelectronic applications. *J. Alloy. Compd.* **2021**, *873*, 159875. [[CrossRef](#)]
8. Feng, Y.; Jiao, T.; Yin, J.; Zhang, L.; Zhang, L.; Zhou, J.; Peng, Q. Facile Preparation of Carbon Nanotube-Cu₂O Nanocomposites as New Catalyst Materials for Reduction of P-Nitrophenol. *Adv. Mater.* **2019**, *14*, 78.
9. Abdelfatah, M.; Ismail, W.; El-Shafai, N.M.; El-Shaer, A. Effect of thickness, bandgap, and carrier concentration on the basic parameters of Cu₂O nanostructures photovoltaics: Numerical simulation study. *Mater. Technol.* **2020**, *36*, 1–9. [[CrossRef](#)]
10. Chandraker, S.K.; Lal, M.; Ghosh, M.K.; Tiwari, V.; Ghorai, T.K.; Shukla, R. Green synthesis of copper nanoparticles using leaf extract of *Ageratum houstonianum* Mill. and study of their photocatalytic and antibacterial activities. *Nano Express* **2020**, *1*, 010033. [[CrossRef](#)]
11. Kwak, K.; Kim, C. Viscosity of Thermal Conductivity of Copper Oxide Nanofluid Dispersed in Ethylene Glycol Viscosity and thermal conductivity of copper oxide nanofluid dispersed in ethylene glycol. *Korea-Aust. Rheol. J.* **2005**, *17*, 35–40.
12. Rehana, D.; Mahendiran, D.; Kumar, R.S.; Rahiman, A.K. Evaluation of antioxidant and anticancer activity of copper oxide nanoparticles synthesized using medicinally important plant extracts. *Biomed. Pharmacother.* **2017**, *89*, 1067–1077. [[CrossRef](#)]
13. Elemike, E.E.; Onwudiwe, D.C.; Singh, M. Eco-friendly synthesis of copper oxide, zinc oxide and copper oxide–zinc oxide nanocomposites, and their anticancer applications. *Journal of Inorganic and Organometallic Polymers and Materials.* **2020**, *30*(2), 400–409. [[CrossRef](#)]
14. Derbalah, A.; Abdelsalam, I.; Behiry, S.I.; Abdelkhalek, A.; Abdelfatah, M.; Ismail, S.; Elsharkawy, M.M. Copper oxide nanostructures as a potential method for control of zucchini yellow mosaic virus in squash. *Pest Manag. Sci.* **2022**, *78*, 3587–3595. [[CrossRef](#)]
15. Salah, H.Y.; Mahmoud, K.R.; Ismail, W.; El-Shaer, A.; Oraby, A.H.; Abdelfatah, M.; EL-Henawey, M.I. Influence of Nickel Concentration on the Microstructure, Optical, Electrical, and Photoelectrochemical Properties of ZnO Nanorods Synthesized by Hydrothermal Method. *J. Electron. Mater.* **2022**, *51*, 910–920. [[CrossRef](#)]
16. Oprea, O.; Andronescu, E.; Ficai, D.; Ficai, A.; Oktar, F.N.; Yetmez, M. ZnO Applications and Challenges. *Curr. Org. Chem.* **2014**, *18*, 192–203. [[CrossRef](#)]
17. Unsoy, G.; Gunduz, U.; Oprea, O.; Ficai, D.; Sonmez, M.; Radulescu, M.; Alexie, M.; Ficai, A. Magnetite: From Synthesis to Applications. *Curr. Top. Med. Chem.* **2015**, *15*, 1622–1640. [[CrossRef](#)]
18. Sankar, R.; Manikandan, P.; Malarvizhi, V.; Fathima, T.; Shivashangari, K.S.; Ravikumar, V. Green synthesis of colloidal copper oxide nanoparticles using *Carica papaya* and its application in photocatalytic dye degradation. *Spectrochim. Acta—Part A Mol. Biomol. Spectrosc.* **2014**, *121*, 746–750. [[CrossRef](#)]
19. El-Shafai, N.M.; Ibrahim, M.M.; Abdelfatah, M.; Ramadan, M.S.; El-Mehasseb, I.M. Synthesis, characterization, and cytotoxicity of self-assembly of hybrid nanocomposite modified membrane of carboxymethyl cellulose/graphene oxide for photocatalytic antifouling, energy storage, and supercapacitors application. *Colloids Surf. A Physicochem. Eng. Asp.* **2021**, *626*, 127035. [[CrossRef](#)]
20. Devi, H.S.; Singh, T.D. Synthesis of Copper Oxide Nanoparticles by a Novel Method and its Application in the Degradation of Methyl Orange. *Adv. Electron. Electr. Eng.* **2014**, *4*, 83–88.
21. Haq, S.; Yasin, K.A.; Rehman, W.; Waseem, M.; Ahmed, M.N.; Shahzad, M.I.; Shahzad, N.; Shah, A.; Rehman, M.U.; Khan, B. Green Synthesis of Silver Oxide Nanostructures and Investigation of Their Synergistic Effect with Moxifloxacin Against Selected Microorganisms. *J. Inorg. Organomet. Polym. Mater.* **2020**, *31*, 1134–1142. [[CrossRef](#)]
22. Altikatoglu, M.; Attar, A.; Erçi, F.; Cristache, C.M.; Isildak, I. Green synthesis of copper oxide nanoparticles using *ocimum basilicum* extract and their antibacterial activity. *Fresenius Environ. Bull.* **2017**, *25*, 7832–7837.

23. Sharma, M.; Singh, J.; Hazra, S.; Basu, S. Adsorption of heavy metal ions by mesoporous ZnO and TiO₂@ZnO monoliths: Adsorption and kinetic studies. *Microchem. J.* **2019**, *145*, 105–112. [[CrossRef](#)]
24. Zhao, X.; Lv, L.; Pan, B.; Zhang, W.; Zhang, S.; Zhang, Q. Polymer-supported nanocomposites for environmental application: A review. *Chem. Eng. J.* **2011**, *170*, 381–394. [[CrossRef](#)]
25. Iravani, S. Green synthesis of metal nanoparticles using plants. *Green Chem.* **2011**, *13*, 2638–2650. [[CrossRef](#)]
26. Keabadile, O.P.; Aremu, A.O.; Elugoke, S.E.; Fayemi, O.E. Green and traditional synthesis of copper oxide nanoparticles—comparative study. *Nanomaterials* **2020**, *10*, 2502. [[CrossRef](#)]
27. Hafeez, M.; Arshad, R.; Khan, J.; Akram, B.; Ahmad, M.N.; Hameed, M.U.; Haq, S. Populus ciliata mediated synthesis of copper oxide nanoparticles for potential biological applications. *Mater. Res. Express* **2019**, *6*, 055043. [[CrossRef](#)]
28. Hamid, A.; Haq, S.; Ur Rehman, S.; Akhter, K.; Rehman, W.; Waseem, M.; Ud Din, S.; Zain-ul-Abdin; Hafeez, M.; Khan, A.; et al. Calcination temperature-driven antibacterial and antioxidant activities of fumaria indica mediated copper oxide nanoparticles: Characterization. *Chem. Pap.* **2021**, *75*, 4189–4198. [[CrossRef](#)]
29. Mahfooz-Ur-Rehman, M.; Rehman, W.; Waseem, M.; Shah, B.A.; Shakeel, M.; Haq, S.; Zaman, U.; Bibi, I.; Khan, H.D. Fabrication of Titanium-Tin Oxide Nanocomposite with Enhanced Adsorption and Antimicrobial Applications. *J. Chem. Eng. Data* **2019**, *64*, 2436–2444. [[CrossRef](#)]
30. Shoukat, S.; Rehman, W.; Haq, S.; Waseem, M.; Shah, A. Synthesis and characterization of zinc stannate nanostructures for the adsorption of chromium (VI) ions and photo-degradation of rhodamine 6G. *Mater. Res. Express* **2019**, *6*, 115052. [[CrossRef](#)]
31. Shah, A.; Tauseef, I.; Ali, M.B.; Yameen, M.A.; Mezni, A.; Hedfi, A.; Haleem, S.K.; Haq, S. In-Vitro and In-Vivo Tolerance and Therapeutic Investigations of Phyto-Fabricated Iron Oxide Nanoparticles against Selected Pathogens. *Toxics* **2021**, *9*, 105. [[CrossRef](#)]
32. Rehman, F.U.; Mehmood, R.; Ali, B.M.; Hedfi, A.; MOhammed, A.; Mezni, A.; Rehman, W.; Waseem, M. Bergenia ciliate-Mediated Mixed-Phase Synthesis and Characterization of Silver-Copper Oxide Nanocomposite for Environmental and Biological Applications. *Materials* **2021**, *14*, 6085. [[CrossRef](#)]
33. Song, H.M.; Kim, S.; Lee, B.; Hong, H.; Lee, G. Chemically ordered FePt₃ nanoparticles synthesized by a bimetallic precursor and their magnetic transitions. *J. Mater Chem.* **2009**, *19*, 3677–3681. [[CrossRef](#)]
34. Ahmed, S.; Ahmad, M.; Swami, B.L.; Ikram, S. A review on plants extract mediated synthesis of silver nanoparticles for antimicrobial applications: A green expertise. *J. Adv. Res.* **2016**, *7*, 17–28. [[CrossRef](#)]
35. Yadi, M.; Mostafavi, E.; Saleh, B.; Davaran, S.; Aliyeva, I.; Khalilov, R.; Nikzamir, M.; Nikzamir, N.; Akbarzadeh, A.; Panahi, Y.; et al. Current developments in green synthesis of metallic nanoparticles using plant extracts: A review. *Artif. Cells Nanomed. Biotechnol.* **2018**, *46*, S336–S343. [[CrossRef](#)]
36. Haq, S.; Dildar, S.; Ali, M.B.; Mezni, A.; Hedfi, A.; Shahzad, M.I.; Shahzad, N.; Shah, A. Antimicrobial and antioxidant properties of biosynthesized NiO nanoparticles using *Raphanus sativus* (*R. sativus*) extract. *Mater. Res. Express* **2021**, *8*, 055006. [[CrossRef](#)]
37. Haq, S.; Rehman, W.; Waseem, M.; Shah, A.; Khan, A.R.; Rehman, M.U.; Ahmad, P.; Khan, B.; Ali, G. Green synthesis and characterization of tin dioxide nanoparticles for photocatalytic and antimicrobial studies. *Mater. Res. Express* **2020**, *7*, 025012. [[CrossRef](#)]
38. Haq, S.; Ahmad, P.; Khandaker, M.U.; Faruque, M.R.I.; Rehman, W.; Waseem, M.; Din, S.U. Antibacterial, antioxidant and physicochemical investigations of tin dioxide nanoparticles synthesized via microemulsion method. *Mater. Res. Express* **2021**, *8*, 035013. [[CrossRef](#)]
39. Magdalane, C.M.; Kaviyarasu, K.; Vijaya, J.J.; Siddhardha, B.; Jeyaraj, B. Photocatalytic activity of binary metal oxide nanocomposites of CeO₂ /CdO nanospheres: Investigation of optical and antimicrobial activity. *J. Photochem. Photobiol. B Biol.* **2016**, *163*, 77–86. [[CrossRef](#)]
40. Haq, S.; Abbasi, F.; Ben Ali, M.; Hedfi, A.; Mezni, A.; Rehman, W.; Waseem, M.; Khan, A.R.; Shaheen, H. Green synthesis of cobalt oxide nanoparticles and the effect of annealing temperature on their physicochemical and biological properties. *Mater. Res. Express* **2021**, *8*, 075009. [[CrossRef](#)]